X-621-67-370

NASA TM X-55901

NEUTRAL AIR WAVES IN THE THERMOSPHERE

H. VOLLAND

AUGUST 1967

GODDARD SPACE FLIGHT CENTER
GREENBELT, MARYLAND

NEUTRAL AIR WAVES IN THE THERMOSPHERE

H. Volland*

AUGUST 1967

*On leave from the Astronomical Institues of the University of Bonn, Germany, as a National Academy of Sciences–National Research Council Associates with the National Aeronautics and Space Administration.

Goddard Space Flight Center
Greenbelt, Maryland

CONTENTS

NEUTRAL AIR WAVES IN THE THERMOSPHERE

by

H. Volland

ABSTRACT

Under the influence of gravity, heat conduction, molecular viscosity, Coriolis force and ion drag eight plane characteristic waves obliquely incident on a horizontally stratified atmosphere can propagate, four of them upward and the other four downward. The four pairs of characteristic waves are the well known acoustic-gravity waves, heat conduction waves, and the ordinary and extraordinary viscosity waves. The eigenvalues of the characteristic waves are calculated numerically giving the following main results:

(a) Under the influence of heat conduction acoustic-gravity waves exist in the whole frequency range and at all angles of incidence.

(b) Coriolis force and ion drag make the atmosphere anisotropic with respect to the characteristic waves. Their propagation characteristics at east-to-west and at north-to-south propagation differ from each other.

(c) At the equator upgoing internal gravity waves prefer a predominant west to east path while downgoing heat conduction waves tend to propagate from north to south.

(d) Downgoing internal gravity waves travelling from north to south lose their abnormal behavior under the influence of the Coriolis force and have phase and group velocities the vertical component of which go in the same direction.

NEUTRAL AIR WAVES IN THE THERMOSPHERE

I. INTRODUCTION

It is a well known experience that the air within the lower atmosphere behaves as a heat insulator and is free of molecular friction. The negligibly small heat flow within air is responsible for the adiabatic behavior of acoustic waves and leads to an "adiabatic" velocity of sound

$$C_a = \sqrt{\gamma \mu \overline{T}} \tag{1}$$

in which $\gamma = c_p / c_v$ is the ratio between the specific heats at constant pressure and at constant volume, $\mu = \tilde{R} / M$ is the ratio between the ideal gas constant $\tilde{R}$ and the molecular weight M, and $\overline{T}$ is the mean temperature of air.

In order to estimate the velocity of heat flow within quiet air we use the one dimensional equation of heat conduction

$$\overline{\rho}\, c_v \frac{\partial T}{\partial t} = \kappa \frac{\partial^2 T}{\partial z^2} \tag{2}$$

in which $\overline{\rho}$ is the mean density, κ is the coefficient of heat conductivity, t is the time and z is the altitude coordinate. Replacing t by a characteristic time τ and z by a characteristic length for which we choose the scale height H, equation (2) leads to a velocity of heat transport

$$V_a = \frac{H}{\tau} = \frac{\kappa}{\overline{\rho}\, c_v H} . \tag{3}$$

Using the numerical values at the earth's surface

$$\overline{T} = 273 \ ^\circ K$$

$$\kappa = 1.8 \times 10^2 \sqrt{\overline{T}} = 3.0 \times 10^3 \text{ erg/cm sec } ^\circ\text{K}$$

$$\overline{\rho} = 1.29 \times 10^{-3} \text{ g/cm}^3$$

$$c_v = 7.2 \times 10^6 \text{ erg/g } ^\circ\text{K}$$

$$H = 8 \text{ km}$$

gives a velocity of

$$V_a = 4 \times 10^{-7} \text{ cm/sec}$$

verifying the adiabatic behavior of air at low heights. Since the coefficient of heat conductivity κ only depends on the temperature T the situation reverses completely if we consider the upper atmosphere. At a height of 200 km mean values are

$$\overline{T} = 1000 \ ^\circ\text{K}$$

$$\overline{\rho} = 2.7 \times 10^{-13} \text{ g/cm}^3$$

$$H = 40 \text{ km}$$

yielding from equation (3) a velocity of

$$V_a = 8 \text{ m/sec}$$

which is by no means negligibly small.

The coefficient of molecular viscosity η is proportional to the coefficient of heat conductivity κ and therefore also depends only on the temperature. The

viscosity usually is characterized by the Reynolds number which is defined as

$$R_a = \frac{\bar{\rho} L^2}{\tau \eta}$$

where L and τ are again characteristic length and time. Replacing L by a reciprocal wave number C_a/ω and τ by the period $1/\omega$ of a wave with angular frequency ω and a phase velocity equal to C_a we obtain from equation (1)

$$R_a = \frac{\gamma \bar{p}}{\omega \eta} \tag{4}$$

Here we used the ideal gas equation

$$\bar{p} = \mu \bar{\rho} \bar{T} \tag{5}$$

in order to introduce the mean pressure $\bar{p}$.

By choosing the same numerical values as above, taking (Chapman and Cowling, 1959)

$$\eta = \frac{\kappa}{2.5\, c_v}$$

and considering the angular frequency $\omega = 1\ \text{sec}^{-1}$ we obtain

$$R_a = \begin{cases} 8.5 \times 10^9 & \text{at sea level} \\ 3.8 & \text{at 200 km height.} \end{cases}$$

Thus with respect to the influence of viscosity we again find an entirely different behavior between the lower and the upper atmosphere. The range of turbulence is related to high Reynolds numbers and small Richardson numbers. In heights below 100 km wind shears and thermal instabilities due to the small heat conduction are responsible for turbulent mixing of the different constituents of the atmosphere. In heights above 120 km the air is nearly in diffusive equilibrium as the result of negligibly small turbulence.

In the following paper we consider plane atmospheric waves propagating obliquely through a horizontally stratified atmosphere under the influence of heat conduction, molecular viscosity, ion drag and the Coriolis force. We shall see that within the upper atmosphere three important parameters exist closely related to the parameters C_a, V_a and R_a of equations (1), (3) and (4) which are

$$C = \sqrt{\mu \bar{T}} \quad \text{"isothermal" velocity of sound}$$

$$V = \frac{\kappa}{c_p \bar{\rho} H} \quad \text{heat conduction velocity} \tag{6}$$

$$R = \frac{\bar{p}}{\omega \eta} \quad \text{Reynolds number}$$

Within the lower atmosphere the two well known acoustic-gravity wave modes (one upgoing and one downgoing) exist (Hines, 1960). Their typical phase velocity is C in the high frequency region. Under the influence of heat conduction two new modes are created, called heat conduction waves (Volland, 1967). Their typical phase velocity is V in the low frequency region. Molecular viscosity generates four additional modes, ordinary and extraordinary viscosity waves. Their phase velocity is typically $C/\sqrt{R}$.

In section 2 the eigenvalue equation is derived. Section 3 deals with special analytical solutions within an isothermal atmosphere. The difference in the behavior of the wave modes as compared with the original adiabatic acoustic-gravity waves introduced by Hines (1960) is stressed. In section 4 the general dispersion equation of all 8 modes is discussed in greater detail.

The first numerical calculation of vertical wave motions in the upper atmosphere taking into account heat conduction was made by Harris and Priester (1962) in their famous Harris-Priester-model. Pitteway and Hines

(1963) and Midgley and Liemohn (1966) discussed the influence of heat conduction and molecular viscosity on the acoustic-gravity waves. In this paper the properties of all kinds of wave modes within the upper atmosphere are examined.

II. THE EIGENVALUE EQUATION

We start from the equations of conservation of mass, momentum and energy and the ideal gas equation of the neutral gas which are

$$\frac{\partial \rho}{\partial t} + \operatorname{div}(\rho \vec{v}) = 0$$

$$\rho \frac{d\vec{v}}{dt} + \operatorname{div} \sigma + \nu \rho (\vec{v} - \vec{v}_i) - 2\vec{\Omega} \times \vec{v} + \operatorname{grad} p - \rho \vec{g} = 0 \tag{7}$$

$$c_v \rho \frac{dT}{dt} + p \operatorname{div} \vec{v} + \beta - \operatorname{div}(\kappa \operatorname{grad} T) = 0$$

$$p - \mu \rho T = 0.$$

ρ density; $\vec{v} = (u,v,w)$ velocity

p pressure; T temperature

ν number of collisions between neutral molecules and ions

σ viscous stress tensor

$$\sigma_{ik} = -\eta \left\{ \frac{\partial v_i}{\partial x_k} + \frac{\partial v_k}{\partial x_i} - \frac{2}{3} \sigma_{ik} \operatorname{div} \vec{v} \right\} \text{ element of } \sigma$$

η coefficient of molecular viscosity

$\vec{\Omega}$ earth's rotational vector

$\vec{g}$ gravitational acceleration force

c_v specific heat at constant volume

$$\vec{v}_i = \frac{(\vec{v} \cdot \vec{B}_0)\,\vec{B}_0}{B_0^2}$$

ion velocity, supposed to be zero when orthogonal to the geomagnetic field $\vec{B}_0$

$$\beta = \sum_i \sum_k \sigma_{ik} \frac{\partial v_i}{\partial x_k}$$

viscosity heating

κ coefficient of heat conductivity

$\mu = \tilde{R}/M$

$\tilde{R}$ gas constant

M molecular weight

For solving the system of equations (7) a consequent perturbation method is applied assuming that the time independent mean values like density $\overline{\rho}$, pressure $\overline{p}$ and temperature $\overline{T}$ are already known and that the mean velocity of the air $\overline{\vec{v}}$ is zero. The perturbation is considered to be a plane harmonic wave of angular frequency ω and of wave number k obliquely incident on a horizontally stratified plane atmosphere in which all parameters depend only on the vertical component z. Then all variables are functions of the coordinates x, y, z, and time t according to

$$f(z)\, e^{j\omega t - jk \sin\theta\,(x \cos\Lambda + y \sin\Lambda)}. \qquad (8)$$

θ is the angle of incidence and Λ is the azimuth of the plane of incidence of the wave with respect to geographic south. We assume that no internal energy source exists. Therefore, the vertical component of energy transported by the different wave modes is continuous at any internal boundary. This implies Snell's law:

$$k \sin \theta = k_0 \sin \theta_0 = \text{const.}$$

$$\Lambda = \Lambda_0 = \text{const.} \tag{9}$$

It is possible, therefore, to relate wavenumber k, angle of incidence θ and azimuth Λ of a wave to an arbitrary wave with wavenumber $k_0 = \omega/C_0$ and angle of incidence θ_0 at the arbitrary height z_0 travelling in the Λ_0 direction. We choose as such an arbitrary wave an undissipated acoustic wave which has in the frequency limit $\omega \to \infty$ within a loss free atmosphere the isothermal acoustic phase velocity $C_0 = \sqrt{\mu T_0}$ of equation (6) and the real wave number k_0. The angle of incidence of this wave is real. C_0 plays the role of a reference velocity equivalent to the velocity of light in the electromagnetic wave propagation in plasma.

For convenience we rotate the coordinate system in such a manner that the new x-axis points in the Λ_0 direction. Then the horizontal components of the velocity with respect to the new coordinate system are

$$\tilde{u} = u \cos \Lambda_0 + v \sin \Lambda_0$$

$$\tilde{v} = -u \sin \Lambda_0 + v \cos \Lambda_0 .$$

The values $\tilde{u}$, $\tilde{v}$, w, Δp, $\Delta \rho$ and ΔT are the deviations from the mean values and are considered to be small compared with $\bar{p}(z)$, $\bar{\rho}(z)$ and $\bar{T}(z)$ of the quiet atmosphere. Thus all products of these small values can be neglected. We normalize these variables according to

$$e_1 = \frac{w}{C_0}; \quad e_3 = \frac{\Delta T}{\bar{T}}; \quad e_5 = \frac{\tilde{u}}{C_0}; \quad e_7 = \frac{\tilde{v}}{C_0}$$

$$e_2 = \frac{\Delta p}{\bar{p}}; \quad e_4 = \frac{\kappa \Delta T'}{C_0 \bar{p}}; \quad e_6 = \frac{\tilde{u}'}{\omega}; \quad e_8 = \frac{\tilde{v}'}{\omega} \tag{10}$$

The derivation with respect to z has been replaced by a prime ($\partial/\partial z = '$).

Introducing the expressions of equation (10) into the system of equations (7) and considering the time and spatial dependence of equation (8) the variables w'' and $\Delta\rho$ can be eliminated which leads to a system of first order differential equations which in concise matrix form is

$$\mathbf{e}' - jk_0 \mathbf{K}\mathbf{e} = \mathbf{0}, \tag{11}$$

where

$$\mathbf{e}(z) = \begin{pmatrix} e_1 \\ \cdot \\ \cdot \\ \cdot \\ e_8 \end{pmatrix}$$

is the row matrix containing the 8 independent variables defined in equation (10). The coefficient matrix

$$\mathbf{K} = \begin{pmatrix} \mathbf{K}_1 & \mathbf{K}_2 \\ \mathbf{K}_3 & \mathbf{K}_4 \end{pmatrix} \tag{12}$$

has the submatrices

$$\mathbf{K}_1 = \begin{pmatrix} -2jA_1 & -1 & 1 & 0 \\ -(1-\delta D)\,d_1 & 2jA_1\delta & -2jA & -\dfrac{jG\delta}{d_2} \\ 0 & 0 & 2jA_2 & -\dfrac{jG}{d_2} \\ -2jd_2\left(A_1 - \dfrac{A}{\gamma}\right) & -1 & d_2\left(1 - \dfrac{jS_0^2}{G}\right) & -2jA \end{pmatrix}$$

$$\mathbf{K}_2 = \begin{pmatrix} S_0 & 0 & 0 & 0 \\ -\delta\left(2A_1 S_0 j + \dfrac{3}{4}RB_1 d_1\right) & -\dfrac{3S_0\delta j}{4} & -\dfrac{3R\delta B_4 d_1}{4} & 0 \\ 0 & 0 & 0 & 0 \\ 0 & 0 & 0 & 0 \end{pmatrix}$$

$$\mathbf{K}_3 = \begin{pmatrix} 0 & 0 & 0 & 0 \\ \left(\dfrac{2}{3}S_0 A_1 - jRB_2 d_1\right) & -S_0 R\left(1 + \dfrac{j}{3R}\right) & j\dfrac{S_0}{3} & 0 \\ 0 & 0 & 0 & 0 \\ -jRB_3 d_1 & 0 & 0 & 0 \end{pmatrix}$$

$$\mathbf{K}_4 = \begin{pmatrix} 0 & -j & 0 & 0 \\ Rd_1(1 - jB_7) - jS_0^2 & 0 & jRB_6 d_1 & 0 \\ 0 & 0 & 0 & -j \\ -jRB_5 d_1 & 0 & Rd_1(1 - jB_8) - jS_0^2 & 0 \end{pmatrix}$$

Here the following abbreviations have been used:

$$k_0 = \frac{\omega}{C_0} \qquad C_0 = \sqrt{\mu \bar{T}}\,/_{z=z_0}$$

$$S_0 = \sin \theta_0 \qquad C = \sqrt{\mu \bar{T}(z)}$$

$$A = \frac{1}{2k_0 H} \qquad H = \frac{\mu \bar{T}}{g} = -\frac{\bar{p}}{\bar{p}'}$$

$$A_1 = \frac{1}{2k_0 H_1} \qquad H_1 = -\frac{\bar{\rho}}{\bar{\rho}'}$$

$$A_2 = \frac{1}{2k_0 H_2} \qquad H_2 = \frac{\bar{T}}{\bar{T}'}$$

$$G = \frac{2AC_0}{V} \qquad V = \frac{\kappa}{c_p \bar{\rho} H}$$

$$d_1 = \frac{C_0^2}{C^2} \qquad d_2 = \frac{\gamma}{(\gamma - 1)}$$

$$\gamma = \frac{c_p}{c_v} \qquad R = \frac{\bar{p}}{\omega \eta}$$

$$\delta = \frac{1}{1 - \frac{3}{4} jR} \; ; \; Z_1 = \frac{2\Omega}{\omega} \; ; \; Z_2 = \frac{\nu}{\omega}$$

$$D = 1 + \frac{3}{4} R Z_2 \cos^2 I + \frac{1}{d_1} \left(\frac{3}{4} S_0^2 - 4A_1^2 - \frac{2A_1'}{k_0} \right)$$

$$\left.\begin{matrix} B_1 \\ B_2 \end{matrix}\right\} = Z_1 \sin \vartheta \sin \Lambda_0 \pm Z_2 \sin I \cos I \cos \Lambda_0$$

$$\left.\begin{matrix} B_3 \\ B_4 \end{matrix}\right\} = Z_1 \sin \vartheta \cos \Lambda_0 \pm Z_2 \sin I \cos I \sin \Lambda_0$$

$$\left.\begin{matrix} B_5 \\ B_6 \end{matrix}\right\} = Z_1 \cos \vartheta \pm Z_2 \cos^2 I \cos \Lambda_0 \sin \Lambda_0$$

$$\left.\begin{matrix} B_7 \\ B_8 \end{matrix}\right\} = Z_2 \left(1 - \cos^2 I \left\{ \begin{matrix} \cos^2 \Lambda_0 \\ \sin^2 \Lambda_0 \end{matrix} \right\} \right)$$

$$\cos I = \frac{\sin \vartheta}{\sqrt{1 + 3 \cos^2 \vartheta}} \qquad \sin I = \frac{2 \cos \vartheta}{\sqrt{1 + 3 \cos^2 \vartheta}}$$

ϑ geographical co-latitude

I geomagnetic dipangle

Λ_0 azimuth

In this calculation the geomagnetic field has been approximated by a dipole field with its axis parallel to the earth's rotational axis. Moreover, the derivatives of μ, κ and η with respect to z have been neglected.

In order to solve equation (11) uniquely it is necessary to know the conditions at the upper or lower boundary of the model atmosphere. Physically appropriate solutions need the separation between upgoing and downgoing waves at these boundaries. Such waves are the characteristic waves which are defined by the

eigen values q_ν of the matrix **K**. They can be found from the eigenvalue equation

$$|\mathbf{K} - \lambda_\nu \mathbf{E}| = 0, \tag{13}$$

with

$$\lambda_\nu = -(q + jA)$$

and

$$\mathbf{E} \text{ unit matrix.}$$

Now a characteristic wave has the z-dependence

$$f_\nu(z) = e^{jk_0\lambda_\nu z} = e^{-jk_0 q_\nu z + \frac{z}{2H}}. \tag{14}$$

Here the real exponential factor $1/2H = k_0 A$ has been split from the eigenvalue q_ν merely because of convenience. It gives the increase of the amplitude with height of a non-dissipative wave in an isothermal atmosphere. Therefore the imaginary term of q_ν is negative or zero for an upgoing wave.

A characteristic wave is uncoupled from the other waves if the elements of the matrix **K** and therefore the q_ν are height independent. Since **K** depends on V and R which themselves depend on $\overline{\rho}$ and $\overline{p}$, respectively, the characteristic waves are always coupled in a realistic atmosphere. Therefore, in order to find out the relative importance of the different wave modes one has to solve the system of equations (7) by numerical methods beginning at an arbitrary level z_0 and integrating upwards (or downwards) to a second arbitrary level z_n (see figure 1). This leads to a solution of the general form

$$\mathbf{e}(z_n) = \mathbf{T}_{z_0}^{z_n}\, \mathbf{e}(z_0). \tag{15}$$

The physical quantities $\mathbf{e}(z_0)$ and $\mathbf{e}(z_n)$ at the boundaries are connected with the characteristic waves by the equation

$$\mathbf{e} = \mathbf{P}\,\mathbf{c}\,. \tag{16}$$

Here

$$\mathbf{c} = \begin{pmatrix} a_1 \\ \cdot \\ \cdot \\ \cdot \\ a_4 \\ b_1 \\ \cdot \\ \cdot \\ \cdot \\ b_4 \end{pmatrix}$$

is composed of four upgoing waves a_ν and four downgoing waves b_ν while $\mathbf{P}$ has to be chosen in such a manner that

$$\mathbf{P}^{-1}\,\mathbf{K}\,\mathbf{P} = \mathbf{N} = \begin{pmatrix} \lambda_1 & 0 & \cdots & 0 \\ 0 & \ddots & & \vdots \\ \vdots & & \lambda_\nu & \\ & & & 0 \\ 0 & \cdots & 0 & \lambda_8 \end{pmatrix} \tag{17}$$

is the diagonalized normal form of the matrix $\mathbf{K}$.

The elements of the eigen vectors $\mathbf{P}_\nu$ ($\mathbf{P}_\nu$ is the ν^{th} row matrix of $\mathbf{P}$) are determined from the system of linear equations

$$(\mathbf{K} - \lambda_\nu\,\mathbf{E}) \cdot \mathbf{P}_\nu = \mathbf{0}. \tag{18}$$

Finally by well known matrix calculus (Volland, 1968) one obtains from equations (15) and (16) the scattering matrix **M** which is defined by the relation (see figure 1)

$$\begin{pmatrix} \mathbf{b}_0 \\ \mathbf{a}_n \end{pmatrix} = \mathbf{M} \begin{pmatrix} \mathbf{a}_0 \\ \mathbf{b}_n \end{pmatrix}.$$

The scattering matrix completely describes the behavior of the atmosphere with respect to plane atmospheric waves.

If the coupling between the different modes is weak a "ray optics" approximation is valid in which each mode is considered to propagate without coupling with a height dependence according to

$$e^{-jk_0 \int_{z_0}^{z} q(\xi)\, d\xi + \int_{z_0}^{z} \frac{d\xi}{2H(\xi)}} \tag{19}$$

In the complex eigenvalue

$$q_\nu = \alpha_\nu - j\beta_\nu \tag{20}$$

the imaginary part β_ν is responsible for the attenuation of the wave mode in the vertical direction while the real part α_ν is a measure of the phase velocity V_p of the wave:

$$V_p\Big|_\nu = \frac{C_0}{\sqrt{S_0^2 + \alpha_\nu^2}} = \frac{C_0}{n} \tag{21}$$

where n is a real refractive index.

The direction of the wave normal is given by

$$\vartheta_p\Big|_\nu = \operatorname{arctg} \frac{S_0}{\alpha_\nu} \tag{22}$$

while the ray direction can be found from the relation

$$\left.\operatorname{tg}\vartheta_{xg}\right|_{\nu} = -\cos\Lambda_0\,\frac{\partial\alpha_\nu}{\partial S_0} + \frac{\sin\Lambda_0}{S_0}\,\frac{\partial\alpha_\nu}{\partial\Lambda_0}$$

$$\left.\operatorname{tg}\vartheta_{yg}\right|_{\nu} = -\sin\Lambda_0\,\frac{\partial\alpha_\nu}{\partial S_0} - \frac{\cos\Lambda_0}{S_0}\,\frac{\partial\alpha_\nu}{\partial\Lambda_0} \qquad (23)$$

where ϑ_{xg} and ϑ_{yg} are the angles of inclination of the ray components in the (x,z)– and the (y,z)–plane with respect to the z–axis.

The ray propagates with vertical group velocity

$$\left.V_g\right|_{\nu} = \frac{C_0}{\dfrac{\partial(\omega\alpha_\nu)}{\partial\omega} - S_0\,\dfrac{\partial\alpha_\nu}{\partial S_0}} \qquad (24)$$

thus allowing "ray treatment" of the waves in complete analogy to electromagnetic wave propagation (see e.g. Budden, 1961). The WKB-approximation of ray optics is distinguished by a specific normalization of the matrix **P** in such a manner that

$$(\mathbf{P^{-1}\,P'}) = \begin{pmatrix} 0 & \cdot & \cdot \\ \cdot & \ddots & \cdot \\ \cdot & \cdot & 0 \end{pmatrix} \qquad (25)$$

is a matrix in which the diagonal line consists only of zeros. (See e.g. Volland, 1968).

The time averaged vertical component of the energy transported by the ν^{th} wave mode is approximately (see e.g., Eckart, 1960)

$$\left.\overline{S_z}\right|_{\nu} = \frac{1}{2}\left.\overline{\operatorname{Re}\,(pw)}\right|_{\nu} = \frac{1}{4}p_0 w_0\,(g_{1\nu}\,g^*_{2\nu} + g^*_{1\nu}\,g_{2\nu}) \begin{cases} a_\nu\,a^*_\nu \\ b_\nu\,b^*_\nu \end{cases} \qquad (26)$$

where $g_{1\nu}$ and $g_{2\nu}$ are the elements of the two first lines of $\mathbf{P}$ and the star indicates complex conjugate values. In the case of the WKB-approximation the amplitudes $a_\nu a_\nu^*$ and $b_\nu b_\nu^*$ of the different modes are directly comparable.

III. SPECIAL SOLUTIONS OF THE EIGENVALUE EQUATION (ISOTHERMAL ATMOSPHERE)

Numerical calculations showing the relative importance of the different wave modes shall be given in an additional paper. Here we confine ourselves to the discussion of the eigenvalue (or dispersion) equation. In this section a few special cases are considered which lead to analytic solutions of the eigenvalue equation. Such solutions are essential because they allow one to identify the various wave modes in more general cases treated numerically in the subsequent section. For convenience we consider only an isothermal atmosphere. Then $\bar{T}' = 0$ and therefore $A_2 = 0$, $A_1 = A$ and $d_1 = 1$ in $\mathbf{K}$ (equation (11)).

In the case of a wave propagating at the equator ($\vartheta = 90°$) in an east-west direction ($\Lambda_0 = \pm 90°$)

$$B_3 = B_4 = B_5 = B_6 = B_8 = 0$$

and

$$B_1 = B_2 = \pm Z_1$$

$$B_7 = Z_2$$

Then the eigenvalue equation (13) has the form

$$\begin{vmatrix} \mathbf{K}_5 & 0 \\ 0 & \mathbf{K}_6 \end{vmatrix} = 0 \qquad (27)$$

with

$$\mathbf{K}_5 = \left(\begin{array}{cccc|cc} & & & & S_0 & 0 \\ & & & & -\delta\left(2AS_0\, j \pm \frac{3}{4}RZ_1\right) & -\frac{3}{4}S_0\,\delta\, j \\ & \mathbf{K}_1 + \lambda_\nu\, \mathbf{E} & & & 0 & 0 \\ & & & & 0 & 0 \\ \hline 0 & & 0 & 0 & \lambda_\nu & -j \\ \frac{2}{3}S_0\, A \mp jRZ_1 & -S_0R\left(1+\frac{j}{3R}\right) & j\,\frac{S_0}{3} & 0 & R\left(1-\frac{jS_0^2}{R}-jZ_2\right) & \lambda_\nu \end{array}\right) \tag{28}$$

$$\mathbf{K}_6 = \begin{pmatrix} \lambda_\nu & -j \\ R\left(1 - j\,\frac{S_0^2}{R}\right) & \lambda_\nu \end{pmatrix} \tag{29}$$

Now the eigenvalue equation can be separated into

$$|\mathbf{K}_5|\ |\mathbf{K}_6| = 0 \tag{30}$$

which implies

$$|\mathbf{K}_5| = 0$$

or (31)

$$|\mathbf{K}_6| = 0$$

The equation $|\mathbf{K}_6| = 0$ gives the eigenvalues of a transversal type of viscosity wave which we name the extraordinary viscosity wave mode:

$$\lambda_{\nu}^2 + jR\left(1 - j\frac{S_0^2}{R}\right) = 0 \tag{32}$$

or

$$q_{\substack{7\\8}} = \mp j\sqrt{S_0^2 + jR} - jA$$

The upper sign stands for the upgoing wave, the lower sign for the downgoing wave. This wave is a pure transversal wave inasmuch as only the horizontal component $\tilde{v}$ orthogonal to the direction of wave propagation is involved. The wave is heavily attenuated for large values of R and is a purely evanescent one at R = 0. It is completely uncoupled from the other wave modes in this direction of propagation. At vertical incidence its phase velocity is (equation (21)).

$$V_p = \pm\frac{\sqrt{2}\,C_0}{\sqrt{R}} = \pm\sqrt{\frac{2\omega\eta}{\bar{p}}}\,C_0$$

and its group velocity is (equation (24)).

$$V_g = \pm 2\,V_p$$

The remaining equation $|\mathbf{K}_5| = 0$ can be solved analytically for two special cases.

3(a) Small Reynolds numbers ($R \to 0$, $\delta \to 1$)

The equation $|\mathbf{K}_5| = 0$ can be written as

$$(\lambda^2 + S_0^2)^2 \left\{\lambda(\lambda + 2jA) + S_0^2 + \frac{jG}{\gamma}\right\} = 0 \tag{33}$$

and has the solutions

$$\begin{aligned} q_{\substack{1\\2}} &= q_{\substack{5\\6}} = \mp jS_0 - jA \\ q_{\substack{3\\4}} &= \mp j\sqrt{A^2 + S_0^2 + \frac{jG}{\gamma}} \sim \pm \frac{G}{2\gamma A} \mp jA\left(1 + \frac{S_0^2}{2A^2}\right) \end{aligned} \tag{34}$$

where the last approximation is valid in the low frequency region ($A^2 \gg G \gg 1$). The upper sign stands for the upward going waves, the lower sign for the downward going waves. The acoustic-gravity mode (index 1 and 2) and the ordinary viscosity mode (index 5 and 6) are purely evanescent waves while the heat conduction mode (index 3 and 4) has the phase velocity (see equation (21))

$$V_p = \frac{\gamma V}{\sqrt{1 + \frac{V^2 S_0^2 \gamma^2}{C_0^2}}}$$

in the low frequency region which in the case of vertical incidence ($S_0 = 0$) is equal to the phase and group velocity (see equation (3))

$$V_a = \gamma V.$$

Thus the heat conduction wave mode is the only carrier of energy.

The ray direction in the low frequency region depends only slightly on S_0. According to equation (23) the heat conduction mode therefore tends to propagate purely vertically. The amplification factor of the upward going wave is negative and small compared with the factor A in equation (14):

$$-\beta_3 + A \sim -\frac{S_0^2}{2A}$$

showing that part of the energy of the upward going heat conduction wave is converted into internal energy of the surrounding air. The same is true for the downward going component which is attenuated according to

$$-\beta_4 + A \sim 2A$$

a factor twice as large as the attenuation factor of a non dissipative downgoing wave (see equation (16)). The effective attenuation factors of the other wave modes according to equation (32) and (34) do not depend on the earth's gravitational field:

$$\mathrm{Im}\,\lambda_\nu = \beta_\nu - A = \pm S_0 \qquad (\nu = 1, 2, 5, 6, 7, 8)$$

3(b) Large Reynolds numbers $(R \to \infty,\ \delta \to 0,\ R\delta \to 4/3\ j)$

In order to solve this problem we have to transform the matrix $\mathbf{K}_5$ in such a manner that we can split the determinant $|\mathbf{K}_5|$ into two independent determinants:

$$|\mathbf{K}_5| = \begin{vmatrix} \bar{\mathbf{K}}_1 + \lambda \mathbf{E} & \mathbf{0} \\ \mathbf{0} & \mathbf{K}_7 \end{vmatrix}$$

We do this by multiplying the 5th row of $\mathbf{K}_5$ (equation (28)) with

$$\pm \frac{jZ_1}{1 - jZ_2} \quad \text{and} \quad \frac{S_0}{1 - jZ_2}$$

respectively, and add this row to the 1st and 2nd row. Then the off diagonal submatrices of $\mathbf{K}_5$ no longer depend on R_1, and their elements become negligibly small compared with the elements of the matrix $\mathbf{K}_7$ when R goes to infinity. Thus the eigenvalue equation becomes

$$|\mathbf{K}_7| \; |\overline{\mathbf{K}}_1 + \lambda \mathbf{E}| = 0$$

and we find the eigenvalues of the ordinary viscosity mode from $|\mathbf{K}_7| = 0$ as

$$q_{\substack{5\\6}} = \mp j \sqrt{S_0^2 + RZ_2 + jR - jA} \tag{35}$$

while the solution of $|\overline{\mathbf{K}}_1 + \lambda \mathbf{E}| = 0$ is

$$q_{\substack{1\\2}} = \mp \sqrt{a - \sqrt{b}}$$

$$q_{\substack{3\\4}} = \mp \sqrt{a + \sqrt{b}} \tag{36}$$

with

$$a = \frac{1}{2}(F - jG) - A^2 - S_0^2$$

$$b = \frac{1}{4}(F - jG)^2 + \frac{jG}{\gamma}\left\{F - (\gamma - 1)\frac{2AMS_0}{U}\right\}$$

$$M = \pm Z_1 - 2AS_0 \quad ; \quad G = \frac{C_0^2}{\omega VH}$$

$$F = U \mp \frac{Z_1 M}{U} \quad ; \quad A = \frac{C_0}{\omega H}$$

$$U = 1 - jZ_2 \quad ; \quad S_0 = \sin \theta_0$$

$$Z_1 = \frac{2\Omega}{\omega} \quad ; \quad Z_2 = \frac{\nu}{\omega}$$

In figure 2 the real parts α_1 and α_2 of the eigenvalues of the upgoing acoustic-gravity wave and of the heat conduction wave calculated from equation (36) have been plotted versus the sine of the angle of incidence $S_0 = \sin \theta_0$ for different angular frequencies between $\omega = 10^{-5}$ and 10^2 sec^{-1} and for neglected Coriolis force and ion drag ($Z_1 = Z_2 = 0$). The Harris-Priester model 5 at 12^{00} local time and 200 km height (CIRA, 1965) has been chosen as the atmospheric model. For convenience the ordinate α is given in two different scales separated by a dash-dotted line, respectively. Because of equation (36) the eigenvalues of the downgoing waves differ only in sign from the eigenvalues of the upgoing waves.

In figure 2a the characteristic behavior of the acoustic-gravity waves can be seen which in the low frequency range ($\omega < 10^{-2}$ sec^{-1}) has a downward direction of phase propagation while the energy of the wave propagates upward. This behavior can be derived from equations (22) and (23) in which the angles of the direction of the wave normal and of the ray (in our special case the ray direction does not depend on Λ_0) are given as:

$$\operatorname{tg} \vartheta_p = \frac{S_0}{\alpha}$$

$$\operatorname{tg} \vartheta_g = -\frac{\partial \alpha}{\partial S_0}$$

Figure 3a shows the geometry of the vectors of the wave normal and of the ray direction derived from equations (22) and (23) at two frequencies belonging

to an acoustic wave type ($\omega = 10^{-2}$ sec^{-1}) and to an interval gravity wave type ($\omega = 10^{-4}$ sec^{-1}) and illustrates again the reversal of vertical phase and group direction of the internal gravity waves. But contrary to the adiabatic case of zero heat conductivity (see Hines' (1960) fig. 9), the interval gravity waves as well as the acoustic waves, exist within the whole range of S_0. For comparison the adiabatic waves ($\kappa = 0$) at the same frequencies have been drawn in fig. 3a as dashed lines. There exists a continuous transition from the interval gravity wave type to the acoustic wave type again in contrast to the adiabatic case where no wave mode can exist within the frequency range of

$$\frac{C_0}{H}\sqrt{\frac{\gamma - 1}{\gamma}} < \omega < \frac{C_0\sqrt{\gamma}}{2H}$$

At high frequencies the acoustic wave approaches the phase velocity of sound C_0.

The heat conduction modes in fig. 2b only slightly depend on the angle of incidence. These wave modes therefore transport their energy nearly vertically (see fig. 3b). In the low frequency range ($\omega < 10^{-4}$ sec^{-1}) the phase velocity of the heat conduction wave is (see equations (21) and (6))

$$V_p \sim \frac{C_0}{\alpha} \sim V$$

and approaches the heat conduction velocity V. In the high frequency range the heat conduction modes become evanescent.

The dependence of α_1 and α_3 (and therefore of α_2 and α_4) on the parameter of the upper atmosphere at vertical incidence ($S_0 = 0$) has already been shown in a previous paper (Volland, 1967). There are some slight differences in the denoting of the variables in that paper compared with the present paper:

old	notation	new
n_3		α_4
n_4		α_2
β_3		$k_0\beta_4 + 1/2H$
β_4		$k_0\beta_2 + 1/2H$

Moreover the following printed errors should be corrected: In fig. 1a ($z = 400$ km) of (Volland, 1967) the trace of n_4 should be moved upward by a factor of 10, and the element A_{21} of **A** in equation (39) should be read as

$$-j\omega a_{21} (1 - \delta D).$$

Figure 4 gives the imaginary terms $k_0\beta_1$ and $k_0\beta_3$ of the acoustic-gravity mode and of the heat conduction mode. Since according to equation (14) the factor 1/2H has been split from the imaginary terms of q the upgoing waves have increasing amplitudes if $k_0\beta < 1/2H$ and decreasing amplitudes if $k_0\beta > 1/2H$. The last one occurs at $\omega > 10^{-2}$ sec^{-1} for the acoustic-gravity mode. For comparison we note that the adiabatic acoustic-gravity waves have the value $\beta_1 = 0$ over the whole frequency range.

The heat conduction mode has an almost constant amplitude at $\omega < 10^{-3}$ sec^{-1} while at frequencies $\omega > 10^{-1}$ sec^{-1} the wave is attenuated nearly completely after a distance of some km.

Under the influence of the Coriolis force and ion drag the atmosphere behaves like an anistropic medium with respect to neutral air waves. This can be seen from the Λ_0-dependence of the ray direction in equation (23). In our special case of equation (36) the propagation in the east-west direction is different from the propagation in the west-east direction recognized by the change in sign of Z_1. But this difference is rather small. The ion drag tends to decrease the influence of the Coriolis force at very low frequencies as can be seen from equation (36) where at $S_0 = 0$ the factor F has the value

$$F \sim \begin{cases} -\frac{j}{\omega}\left(\nu + \frac{4\Omega^2}{\nu}\right) \\ -\frac{4\Omega^2}{\omega^2} \end{cases} \text{for} \begin{cases} Z_1, Z_2 \gg 1 \\ Z_1 \gg; \; Z_2 = 0 \end{cases} \qquad (37)$$

thus decreasing like ω^{-2} at $Z_2 = 0$ as compared with a decrease like ω^{-1} at $Z_2 \neq 0$.

Because of our assumption that the ion velocity is zero orthogonal to the geomagnetic field lines (see equation (7)) the horizontal ion drag is fully effective for the east-west propagation while for the north-south propagation the horizontal ion drag completely disappears. Because of equation (37) we therefore expect a rather large difference in the behavior between these two directions of propagation. This will be confirmed in the next section.

IV. GENERAL BEHAVIOR OF THE EIGENVALUES

Apart from some special analytical solutions which we gave in the previous section, equation (13) has to be treated by numerical methods. A convenient program available in the SHARE Program Catalog is SAD 3099 (EIG 4) which solves eigenvalues of complex matrices and is coded for the IBM 7090/94. This program has been used for the following calculations.

The atmospheric model is again the Harris-Priester model 5 at 12^{00} local time and 200 km height (CIRA, 1965) which has the data

$$H = 43.3\ \text{km} \quad ; \quad \kappa = 8.64 \times 10^{3}\ \text{erg/cm sec °K}$$

$$\bar{T} = 1100\,°\text{K} \quad ; \quad c_v = 7.23 \times 10^{6}\ \text{erg/g °K}$$

$$\bar{\rho} = 2.71 \times 10^{-13}\ \text{g/cm}^3 \quad ; \quad \gamma = 1.5$$

Moreover the following additional numerical values have been used:

$$\nu = 10^{-4}\ \text{sec}^{-1} \quad ; \quad \vartheta = 90°$$

$$\Omega = 7.23 \times 10^{-5}\ \text{sec}^{-1} \quad ; \quad \Lambda_0 = 90°,\ 180°$$

$$\eta \doteq 4.78 \times 10^{-4}\ \text{g/cm sec}$$

In figures 5 and 6 the calculated real parts of the eigenvalues α_2, α_4, α_6, α_8 of the downward going four wave modes at the equator ($\vartheta = 90°$) have been plotted versus the sine of the angle of incidence $S_0 = \sin \theta_0$ for the different frequencies $\omega = 10^{-5}$ sec^{-1} to 10^{2} sec^{-1}. The full lines give the modes propagating from west to east ($\Lambda_0 = 90°$), the dashed lines are due to the propagation from south to north ($\Lambda_0 = 180°$). Again for convenience the ordinates in figure 5 have different scales divided by the dash-dotted lines. Apart from the acoustic-gravity mode the difference in the behavior between the downgoing and the upgoing waves is rather small. Therefore

$$\alpha_2 \sim -\alpha_4$$

$$\alpha_5 \sim -\alpha_6$$

$$\alpha_7 \sim -\alpha_8$$

within less than 10% accuracy, and the α_2, α_4, α_6 and α_8 are plotted as negative values in order to compare them directly with the values α_1 and α_3 in figure 3.

Likewise the east-west propagation and the west-east propagation on the one hand and the north-south and the south-north propagation on the other hand show nearly the same propagation characteristics. Thus we confine ourselves to downgoing waves propagating from west to east (full lines) and from south to north (dashed lines).

Comparing figure 5 with figure 2 we do not see large differences in the behavior of the acoustic-gravity mode at east-west propagation within the low frequency range ($\omega < 10^{-2}$ sec^{-1}) and in the whole frequency range of the heat conduction modes. This shows that the Reynolds number R which is rather large there ($R > 242$ for $\omega < 10^{-2}$ sec^{-1}) does not influence very much these waves. On the other hand at frequencies $\omega > 1$ sec^{-1} ($R < 0.242$) the acoustic-gravity mode differs strongly from the R-free type in figure 2 giving evidence that in this frequency range the approximation $R \to 0$, treated in section 3(a), begins to be valid. The acoustic wave becomes an evanescent one there.

The striking feature of figure 5a is, however, the behavior of the waves propagating from south to north (the dashed lines in figure 5). Now the gravity modes at $\omega < 10^{-2}$ sec^{-1} have lost their abnormal propagation characteristics and behave in the normal sense with phase and group velocity going in the same vertical direction at angles of incidence $S_0 < 0.9$. This is essentially due to the Coriolis force which is not reduced in its influence by the ion drag at this azimuth of propagation (see equation (37)) as was the case for west to east propagation.

The phase velocity of the heat conduction mode (figure 5b) increases with approach to the north-south propagation at low frequencies. In a ray optics treatment a heat conduction wave travelling downward will shift therefore its direction towards a predominantly north to south direction. This is illustrated in figure 7 where the refractive index surface of the upgoing heat conduction wave

$$n_3 = \sqrt{S_0^2 + \alpha_3^2}$$

has been drawn in a (S_0, Λ_0)-plane. The vector of the ray direction is perpendicular to this surface (see equation (23)) and generally is bent out of the plane of incidence. The ray will laterally deviate during its propagation till it reaches the stable north-south plane where the lateral deviation out of the plane of incidence is zero.

The real parts of the eigenvalues of the ordinary and the extraordinary viscosity waves in figure 6 behave very similar to the heat conduction waves apart from the lowest frequency range.

Figures 8 and 9 show the imaginary parts $k_0\beta_i$ (the attenuation factors) of the downgoing waves at the equator again plotted as negative values in order to compare them with the values in figure 4. Here the azimuth of propagation has no striking influence on the attenuation factors. Thus only the east-west propagation is shown.

While the attenuation factors of the heat conduction waves in figure 8b only slightly differ from the viscosity free mode in figure 4b the acoustic-gravity waves (figure 8a) are heavily attenuated in the high frequency range ($\omega > 1$ sec^{-1} contrary to the viscosity free case. The reason is that in this frequency range $R < 1$, and the approximation $R \to 0$ treated in section 3a can be used which leads to equation (34) and shows that the acoustic waves become evanescent ones.

The attenuation factors of the ordinary viscosity waves in figure 9 look similar to the attenuation factors of the heat conduction waves. But the extraordinary viscosity waves have even positive values of $k_0\beta_8$ at $\omega < 10^{-4}$ sec^{-1}. This results from the fact that according to equation (32) the effective attenuation factor of this wave mode is

$$-\beta_{\substack{7\\8}} + A \sim \mp\left(\sqrt{\frac{R}{2}} \pm A\right) + A = \pm\sqrt{\frac{R}{2}}$$

and does not depend on the earth's gravitation field. If $A > \sqrt{R/2}$ which occurs at $\omega = 10^{-5}$ sec^{-1} β_8 becomes negative.

Figure 10 shows the real part of the eigenvalue α_1 of the upgoing acoustic-gravity mode at the equator. We see that again west-east and north-south propagation differ remarkably in the lowest frequency range though there is not such striking reversal in the propagation characteristics as for the downgoing waves in figure 5. The ray bending as illustrated in figure 7 leads to a predominantly west-east propagation for frequencies between $\omega = 10^{-4}$ and 10^{-2} sec^{-1}.

The same calculations have been repeated for the values $\vartheta = 45°$ and $135°$ equivalent to the geographical latitudes of $\pm 45°$. The results have essentially the same features as figures 5 to 10 but with, of course, different numerical

values. A big difference occurs in the acoustic-gravity mode where the reversal to a normal behavior of the downgoing wave now appears at the west-east propagation path while the north-south propagation acts in the usual way. There exists no large difference in the propagation characteristics between 45° and -45° latitude. The equatorial ray deviation of the heat conduction waves toward a north-south propagation as illustrated in figure 7 is diminished in ±45° latitude. Likewise at heights greater than 200 km the situation does not change completely apart from the fact that with increasing height the Reynolds number decreases. Thus the range where the approximation $R \to 0$ (equation 34) is valid shifts to smaller frequencies and the heat conduction mode tends to remain the only carrier of energy.

V. CONCLUDING REMARKS

It has been shown that eight obliquely incident plane characteristic waves can propagate through a horizontally stratified atmosphere, four of them travelling upwards and the other four travelling downward. The four pairs of characteristic waves are the well known acoustic-gravity waves, the heat conduction waves and ordinary and extraordinary viscosity waves. The heat conduction waves and the viscosity waves are named according to their relation to finite heat conductivity and finite molecular viscosity. Under the influence of the Coriolis force the atmosphere behaves like an anistropic medium with respect to atmospheric waves. Ion drag tends to decrease the influence of the Coriolis force in such a manner that at the equator the west to east propagation path is less effected by the Coriolis force than the north to south propagation path.

Real and imaginary parts of the eigenvalues of the characteristic wave modes have been calculated numerically. With the help of these eigenvalues the general behavior of the different wave modes has been discussed in detail. The main results are the following:

(a) Under the influence of heat conduction there exists a continuous transition from the low frequency range of the acoustic-gravity waves (the so called internal gravity waves) to the real acoustic waves at all angles of incidence. The internal gravity waves are attenuated transferring part of their energy into internal energy of the surrounding air in such a manner that the amplitude of an upgoing wave remains nearly constant.

A new mode – heat conduction waves – is created which shows small dispersion within the low frequency range and which transports its energy mainly vertically. Group and phase velocity have the same direction.

(b) Taking into account molecular viscosity two additional modes – ordinary and extraordinary viscosity waves – exist. Their propagation characteristics are similar to the heat conduction waves.

Molecular viscosity does not change very much the general behavior of the internal gravity waves and of the heat conduction waves but alters the acoustic waves within the high frequency range into evanescent ones.

(c) Coriolis force and ion drag make the atmosphere anisotropic with respect to the characteristic wave modes. At the equator within the low frequency range heat conduction "rays" are laterally deviated out of their plane of incidence toward a predominately north to south direction while internal gravity waves prefer a predominately east to west direction. Travelling ionospheric disturbances show some preferred horizontal directions of propagation depending on season and latitude (Heisler, 1963). This might be due to the influence of the Coriolis force in an atmosphere varying with geographic latitude and season. If this is true it should be possible to decide from the different behavior of the internal gravity waves and of the heat conduction waves in a rotating atmosphere whether upgoing acoustic-gravity waves (Hines, 1960) or downgoing heat conduction waves (Volland, 1967) are responsible for these travelling disturbances.

Downgoing internal gravity waves travelling north to south lose their abnormal behavior under the influence of the Coriolis force and have phase and group velocities the vertical component of which go in the same direction.

The relative importance of the different wave modes for energy transport remains an open question. Because of the coupling of the different modes within a realistic atmosphere this problem can only be solved by a numerical calculation using full wave theory.

In a ray optics treatment one should expect that the time averaged energy transport of each wave mode could be calculated from equation (26). But unfortunately equation (26) is only valid under adiabatic conditions. In a dissipative atmosphere where heat conduction and molecular viscosity must be taken into account the ray direction derived from the wave packet method (equation (23)) differs substantially from the direction of the energy flux vector $p\,\vec{v}$ (of which equation (26) is the vertical component). This situation is equivalent to electromagnetic wave propagation where the Poynting vector shows the same discrepancy with respect to the ray direction (Hines, 1951). The reason for this difference is the fact that the energy flux vector of the atmospheric

waves contains the gravitational potential (Volland, 1967) which is uncertain by a constant factor. The treatment of this problem will be the subject of a forthcoming paper.

ACKNOWLEDGEMENT

I am very indebted to H. G. Mayr for valuable discussions.

REFERENCES

K. G. Budden, "Radio waves in the ionosphere," University Press, Cambridge, 1961.

S. Chapman and T. G. Cowling, "The mathematical treatment of non-uniform gases," University Press, Cambridge, 1959.

CIRA, 1965, "COSPAR international reference atmosphere, 1965," North Holland Publishing Company, Amsterdam, 1965.

C. Eckart, "Hydrodynamics of the oceans and the atmosphere," Pergamon Press, Oxford, London, New York, 1960.

J. Harris and W. Priester, "Time dependent structure of the upper atmosphere," J. Atm. Sci. 19, (1962), 286-301.

L. H. Heisler, "Observation of movement of perturbations in the F-region," Journ. Atm. Terr. Phys. 25, (1963), 71-86.

C. O. Hines, "Wave packets, the Poynting vector and energy flow, Part I to IV," Journ. Geophys. Res. 56, (1951), 63-72, 197-206, 207-220, 535-544.

C. O. Hines, "Internal gravity waves at ionospheric heights," Can. Journ. Phys. 38, (1960), 1441-1481.

J. E. Midgley and H. B. Liehmon, "Gravity waves in a realistic atmosphere," Journ. Geophys. Res. 71, (1966), 3729-3748.

M. L. V. Pitteway and C. O. Hines, "The viscous damping of atmospheric gravity waves," Can. Journ. Phys. 41, (1963), 1935-1948.

H. Volland, "Heat conduction waves in the upper atmosphere," Journ. Geophys. Res. 72, (1967), 2831-2841.

H. Volland, "Die Ausbreitung langer Wellen," Vieweg Verlag, Braunschweig, 1968.

FIGURE CAPTIONS

Figure 1. The upgoing (**a**) and the downgoing (**b**) characteristic waves at the boundaries of an atmospheric model.

Figure 2. Real part α of the eigenvalues of the upgoing acoustic-gravity waves (figure 2a) and of the heat conduction waves (figure 2b) versus the sine of the angle of incidence θ_0 taking into account heat conduction. The parameter is the angular frequency ω (in $\sec^{-1}$). The dash-dotted lines separate different scales.

Figure 3. Illustration of the vector of the real refractive index $\vec{n}$ (which goes in the direction of the wave normal) and the vector of ray direction (which is perpendicular to the refractive index surface) for an internal gravity wave ($\omega = 10^{-4}$ $\sec^{-1}$), for an acoustic wave type ($\omega = 10^{-2}$ $\sec^{-1}$) (figure 3a) and for a heat conduction wave (figure 3b). The dashed lines in figure 3a are the equivalent adiabatic acoustic-gravity waves.

Figure 4. Imaginary part $k_0\beta$ (attenuation factor) of the eigenvalues of the upgoing acoustic-gravity waves (figure 4a) and of the heat conduction waves (figure 4b). The parameter is the angular frequency ω (in $\sec^{-1}$). Waves with values $k_0\beta \lessgtr 1/2H$ have decreasing (increasing) amplitudes with height.

Figure 5. Negative real part $-\alpha$ of the eigenvalues of the downgoing acoustic-gravity waves (figure 5a) and of the downgoing heat conduction waves (figure 5b) versus the sine of the angle of incidence θ_0 taking into account heat conduction, molecular viscosity, Coriolis force and ion drag. The parameter is the angular frequency ω (in $\sec^{-1}$). The propagation conditions are: West to east propagation (full lines) and south to north propagation (dashed lines) at the equator. The dash-dotted lines separate different scales.

Figure 6. Negative real part $-\alpha$ of the eigenvalues of the downgoing ordinary and extraordinary waves. For details see text of figure 5.

Figure 7. Ray refractive index $n_3 = \sqrt{\alpha_3^2 + S_0^2}$ of the upgoing heat conduction wave in a (S_0, Λ_0)-plane illustrating the bending of the ray out of the plane of incidence.

Figure 8. Negative imaginary part $-k_0\beta$ (attenuation factor) of the downgoing acoustic-gravity waves (figure 8a) and of the heat conduction waves (figure 8b) versus sinus of angle of incidence θ_0 taking into account heat conduction, molecular viscosity, Coriolis force and ion drag. The parameter is the angular frequency ω (in sec^{-1}). The propagation conditions are: West to east propagation at the equator.

Figure 9. Negative imaginary part $-k_0\beta$ (attenuation factor) of the downgoing ordinary and extraordinary waves. For details see text of figure 8.

Figure 10. Real part α of the eigenvalue of the upgoing acoustic-gravity waves versus the sine of the angle of incidence θ_0 taking into account heat conduction, molecular viscosity, Coriolis force and ion drag. The parameter is the angular frequency ω (in sec^{-1}). The propagation conditions are: West to east propagation (full lines) and south to north propagation (dashed lines) at the equator. The dash-dotted lines separate different scales.

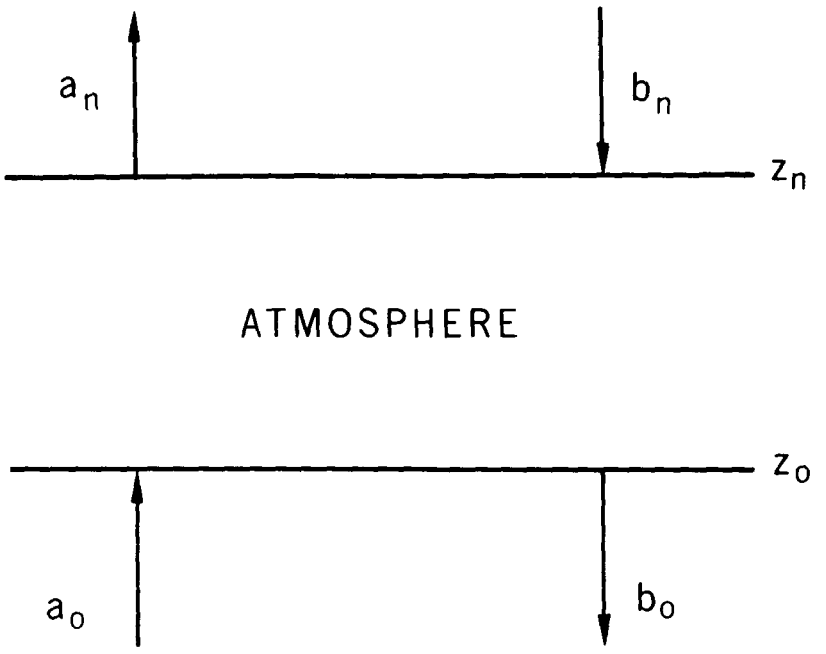

Figure 1—The upgoing (a) and the downgoing (b) characteristic waves at the boundaries of an atmospheric model.

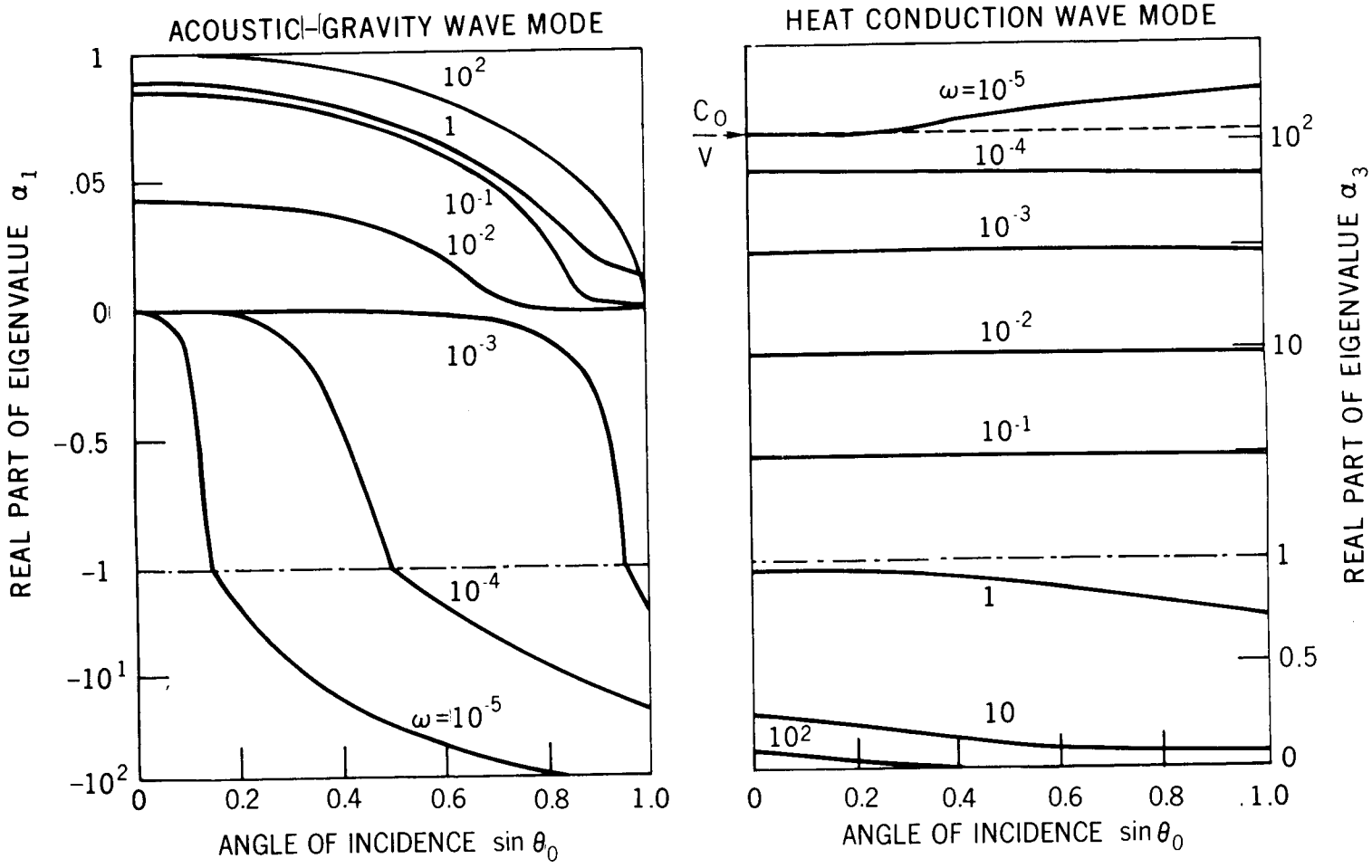

Figure 2–Real part α of the eigenvalues of the upgoing acoustic-gravity waves (figure 2a) and the heat conduction waves (figure 2b) versus the sine of the angle of incidence θ_0 taking into account heat conduction. The parameter is the angular frequency ω (in $\sec^{-1}$). The dash-dotted lines separate different scales.

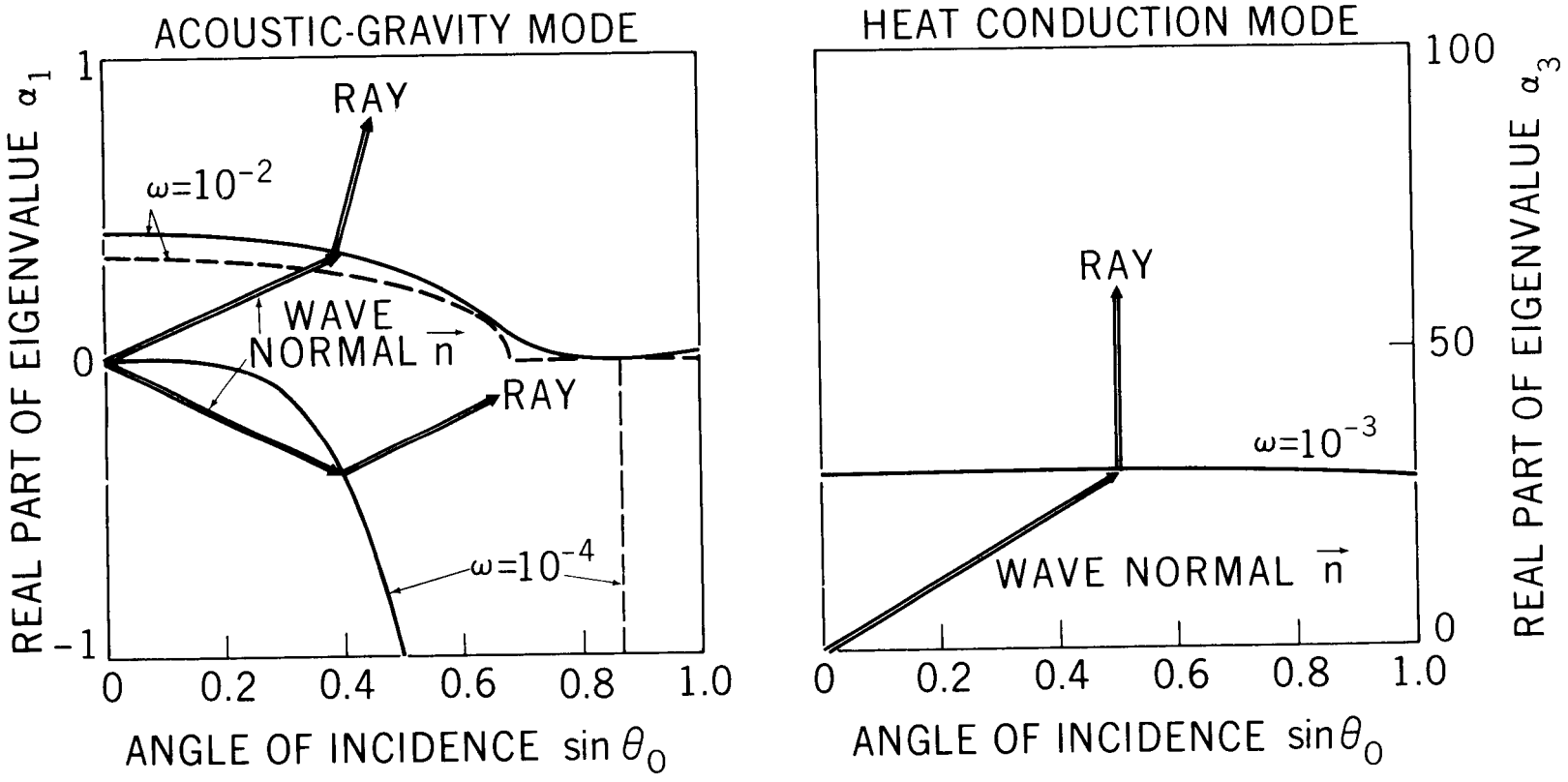

Figure 3–Illustration of the vector of the real refractive index $\vec{n}$ (which goes in the direction of the wave normal) and the vector of ray direction (which is perpendicular to the refractive index surface) for an internal gravity wave ($\omega = 10^{-4}$ sec^{-1}), for an acoustic wave type ($\omega = 10^{-2}$ sec^{-1}) (figure 3a) and for a heat conduction wave (figure 3b). The dashed lines in figure 3a are the equivalent adiabatic acoustic-gravity waves.

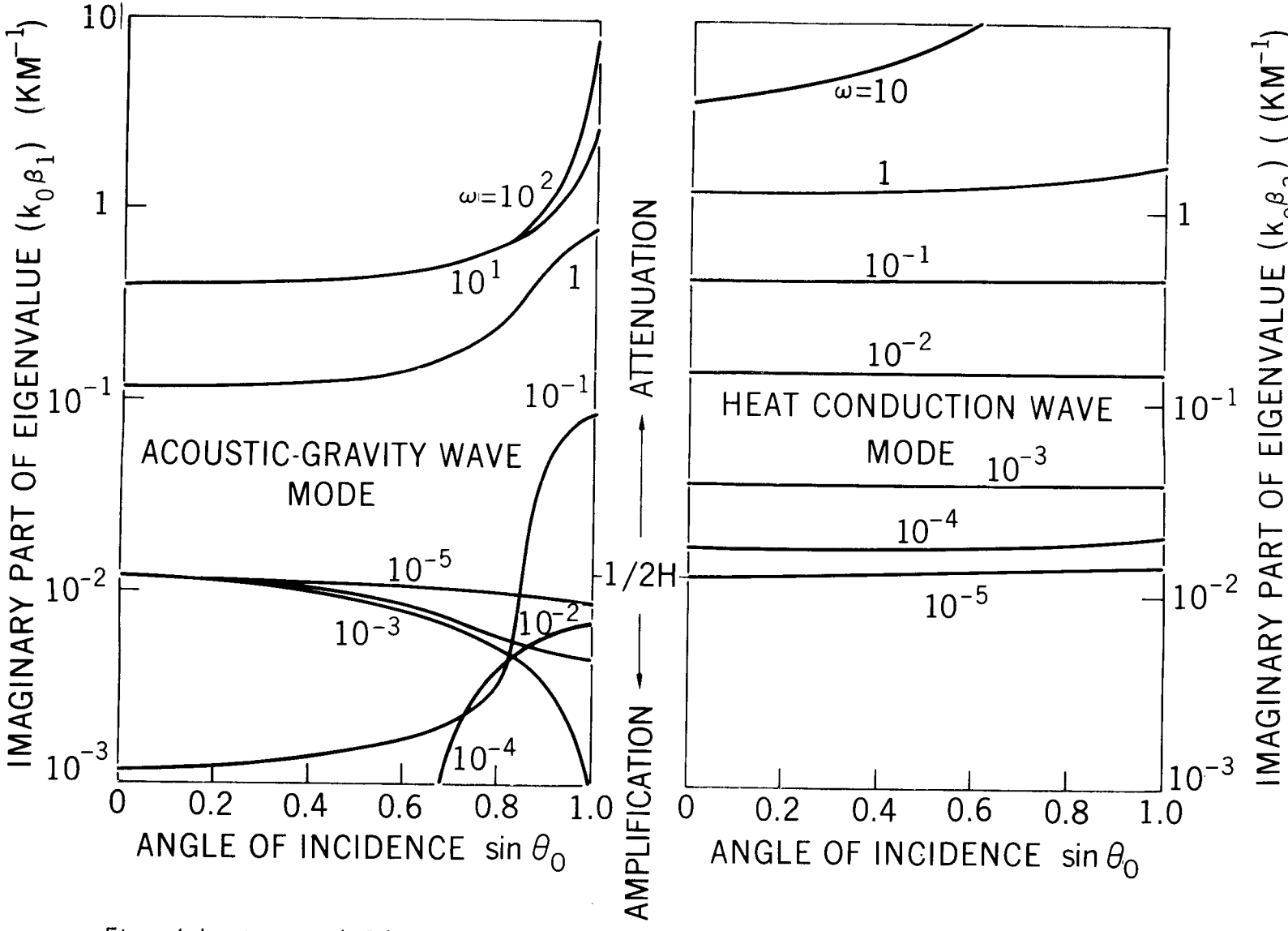

Figure 4–Imaginary part $k_0\beta$ (attenuation factor) of the eigenvalues of the upgoing acoustic-gravity waves (figure 4b) and of the heat conduction waves (figure 4b). The parameter is the angular frequency ω (in sec^{-1}). Waves with values $k_0\beta \lesssim 1/2H$ have decreasing (increasing) amplitudes with height.

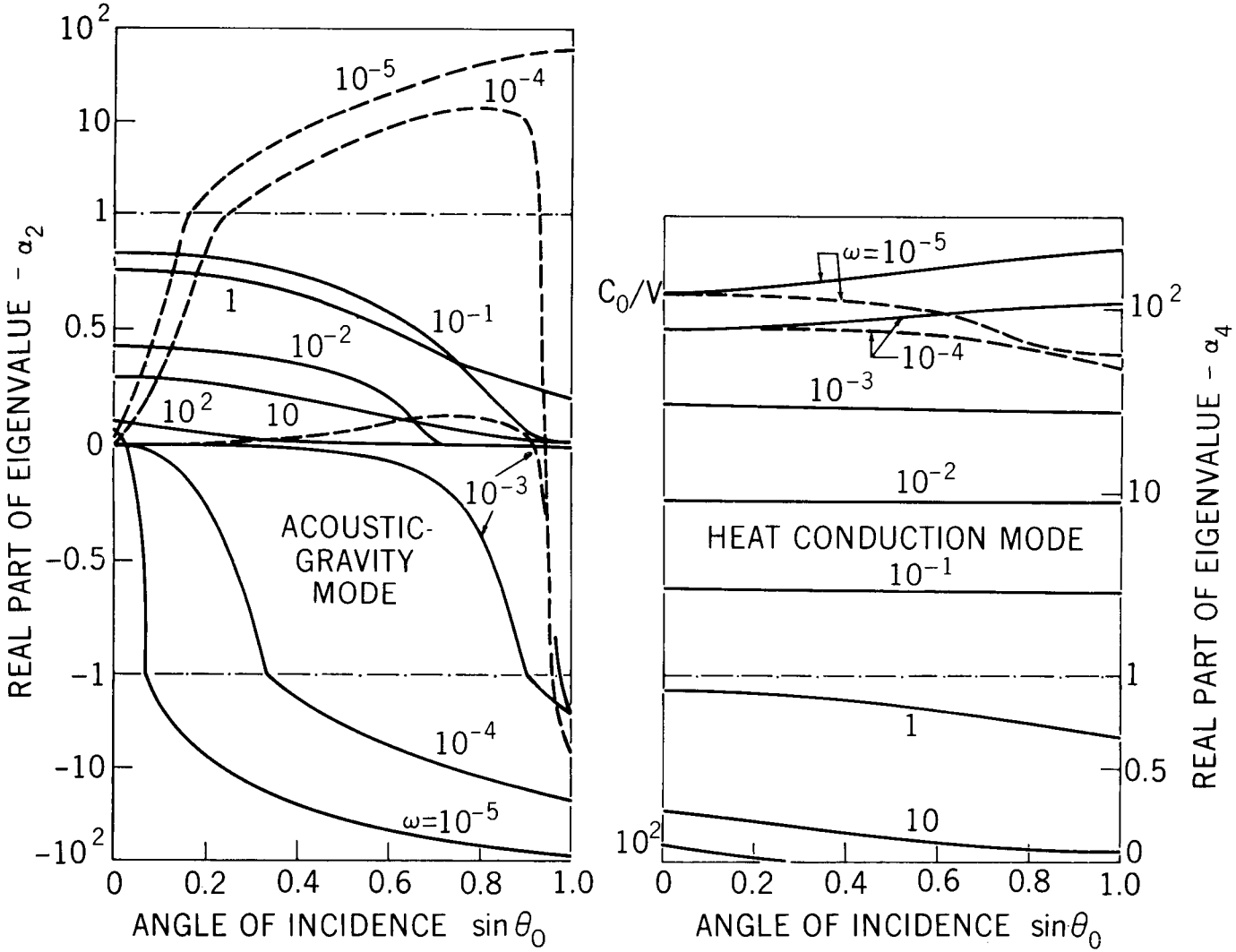

Figure 5–Negative real part $-\alpha$ of the eigenvalues of the downgoing acoustic-gravity waves (figure 5a) and of the downgoing heat conduction waves (figure 5b) versus the sine of the angle of incidence θ_0 taking into account heat conduction, molecular viscosity, Coriolis force and ion drag. The parameter is the angular frequency ω (in $\sec^{-1}$). The propagation conditions are: West to east propagation (full lines) and south to north propagation (dashed lines) at the equator. The dash-dotted lines separate different scales.

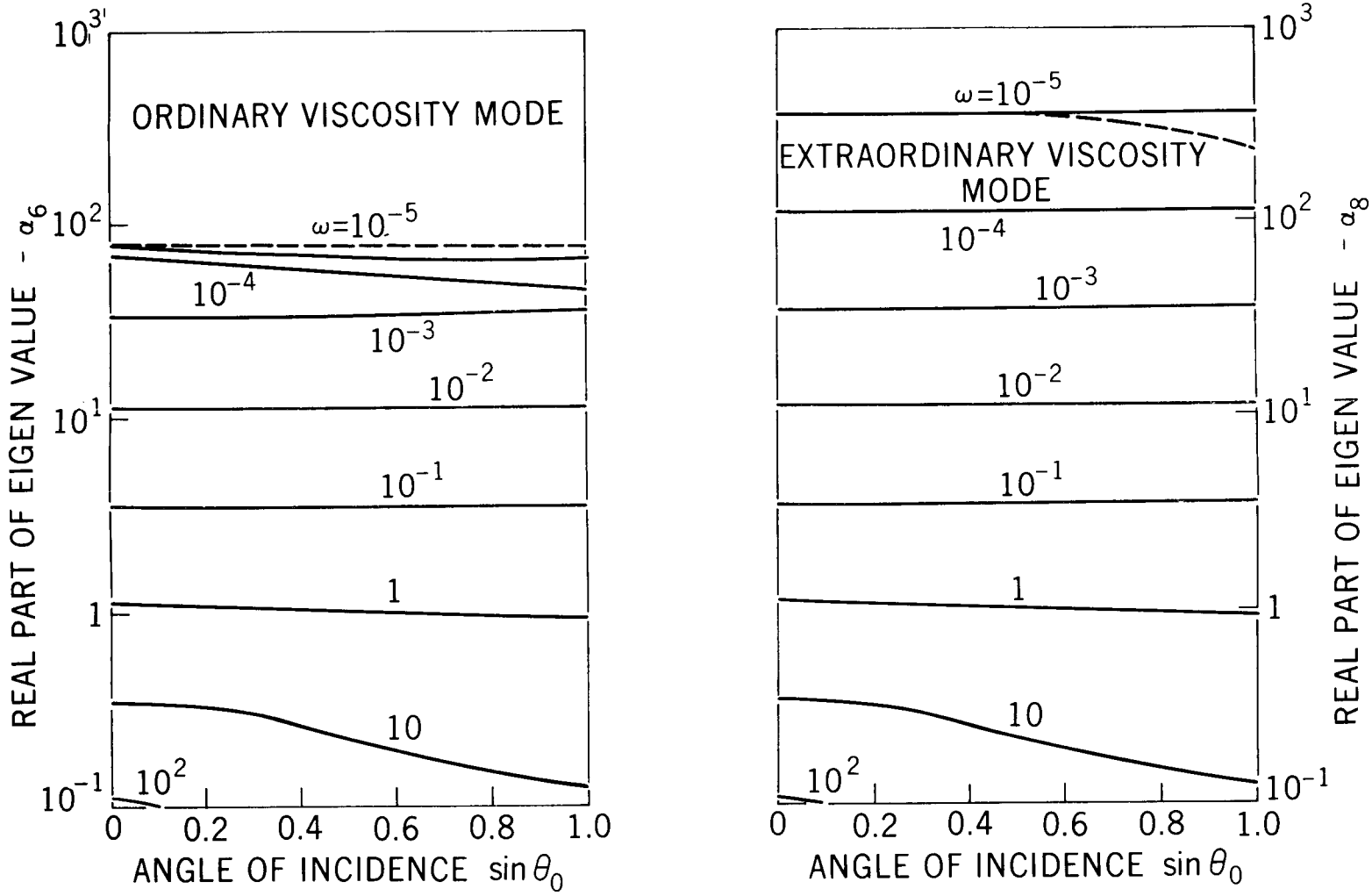

Figure 6–Negative real part $-\alpha$ of the eigenvalues of the downgoing ordinary and extraordinary waves. For details see text of figure 5.

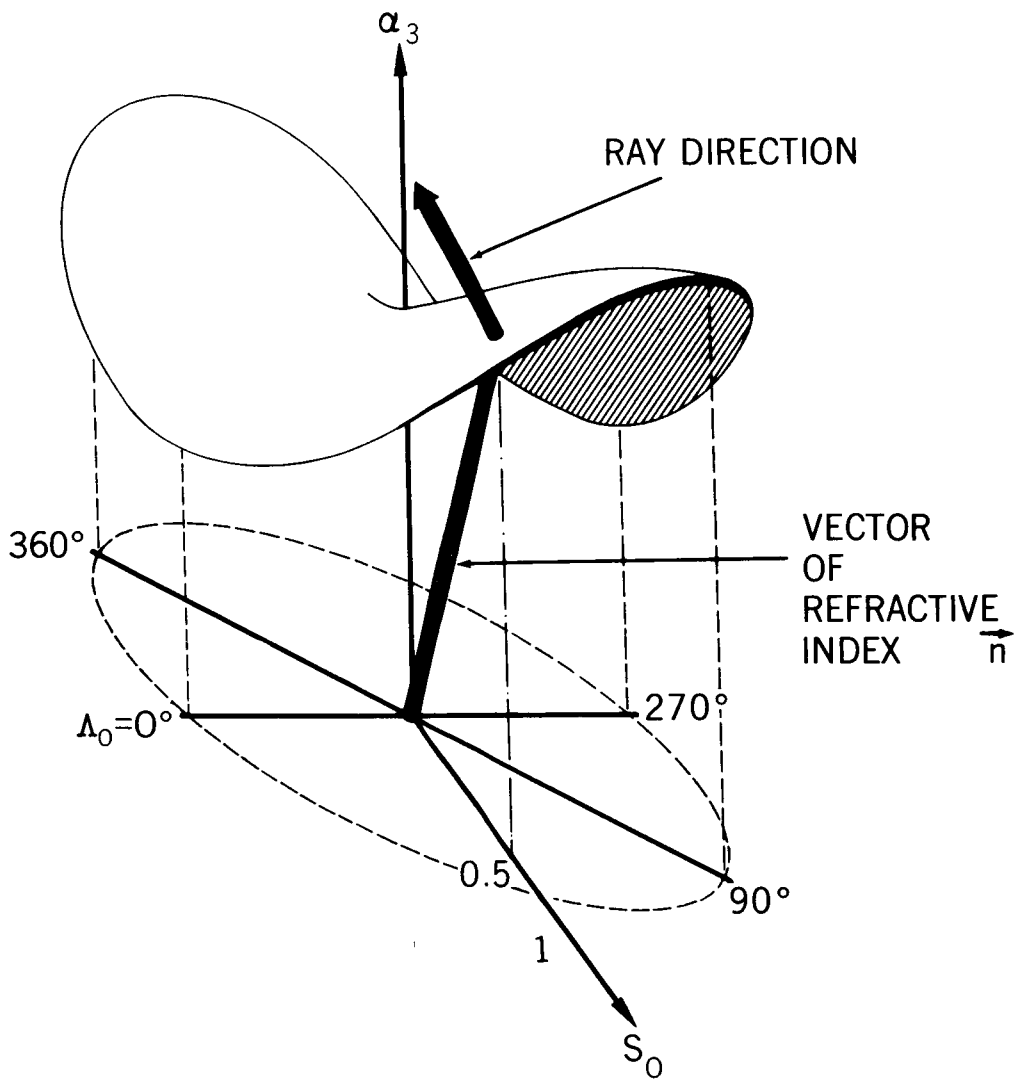

Figure 7–Ray refractive index $n_3 = \sqrt{\alpha_3^2 + S_0^2}$ of the upgoing heat conduction wave in a (S_0, Λ_0)-plane illustrating the bending of the ray out of the plane of incidence.

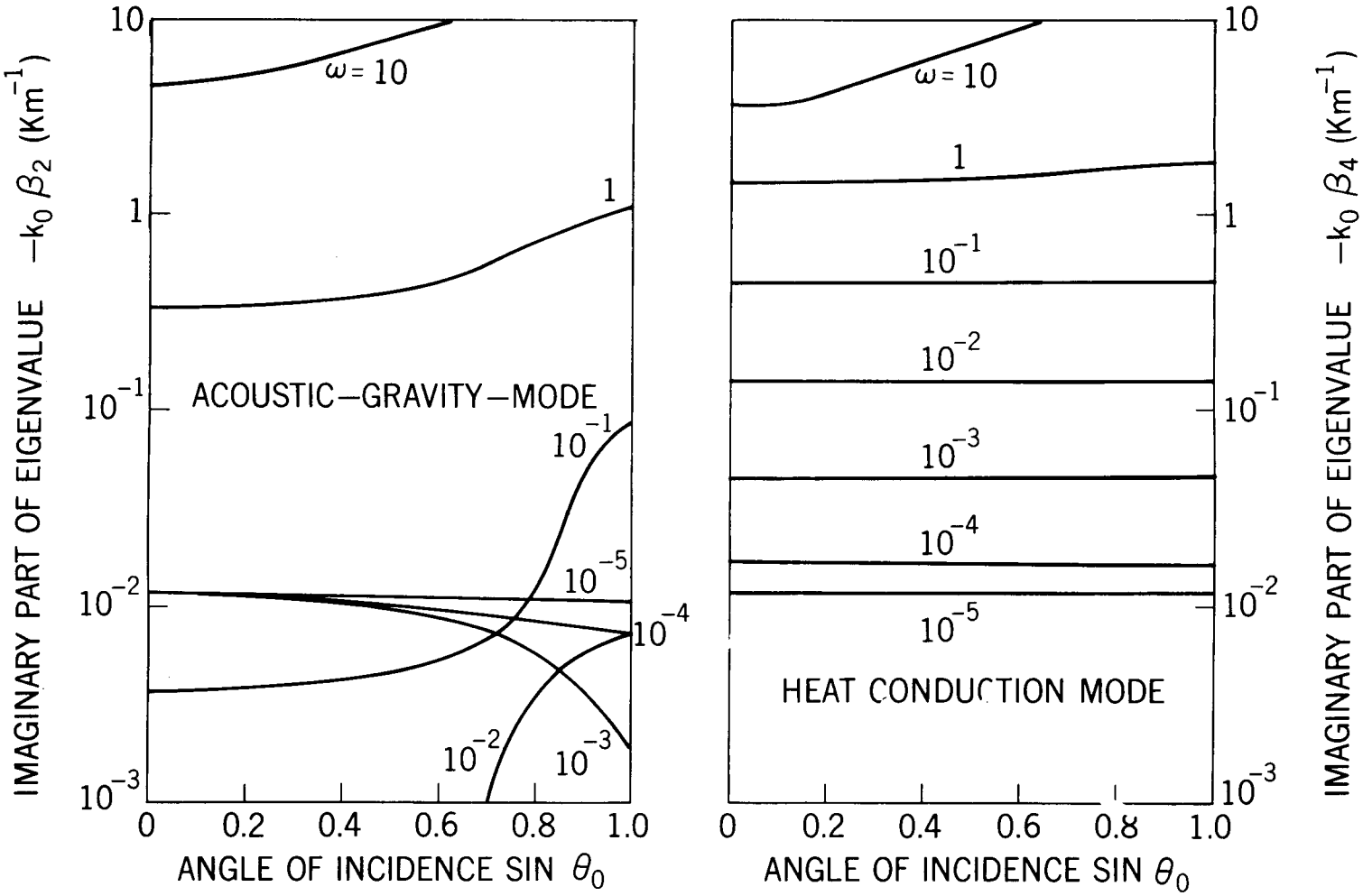

Figure 8–Negative imaginary part $-k_0\beta$ (attenuation factor) of the downgoing acoustic-gravity waves (figure 8a) and of the heat conduction waves (figure 8b) versus sinus of angle of incidence θ_0 taking into account heat conduction, molecular viscosity, Coriolis force and ion drag. The parameter is the angular frequency ω (in sec^{-1}). The propagation conditions are: West to east propagation at the equator.

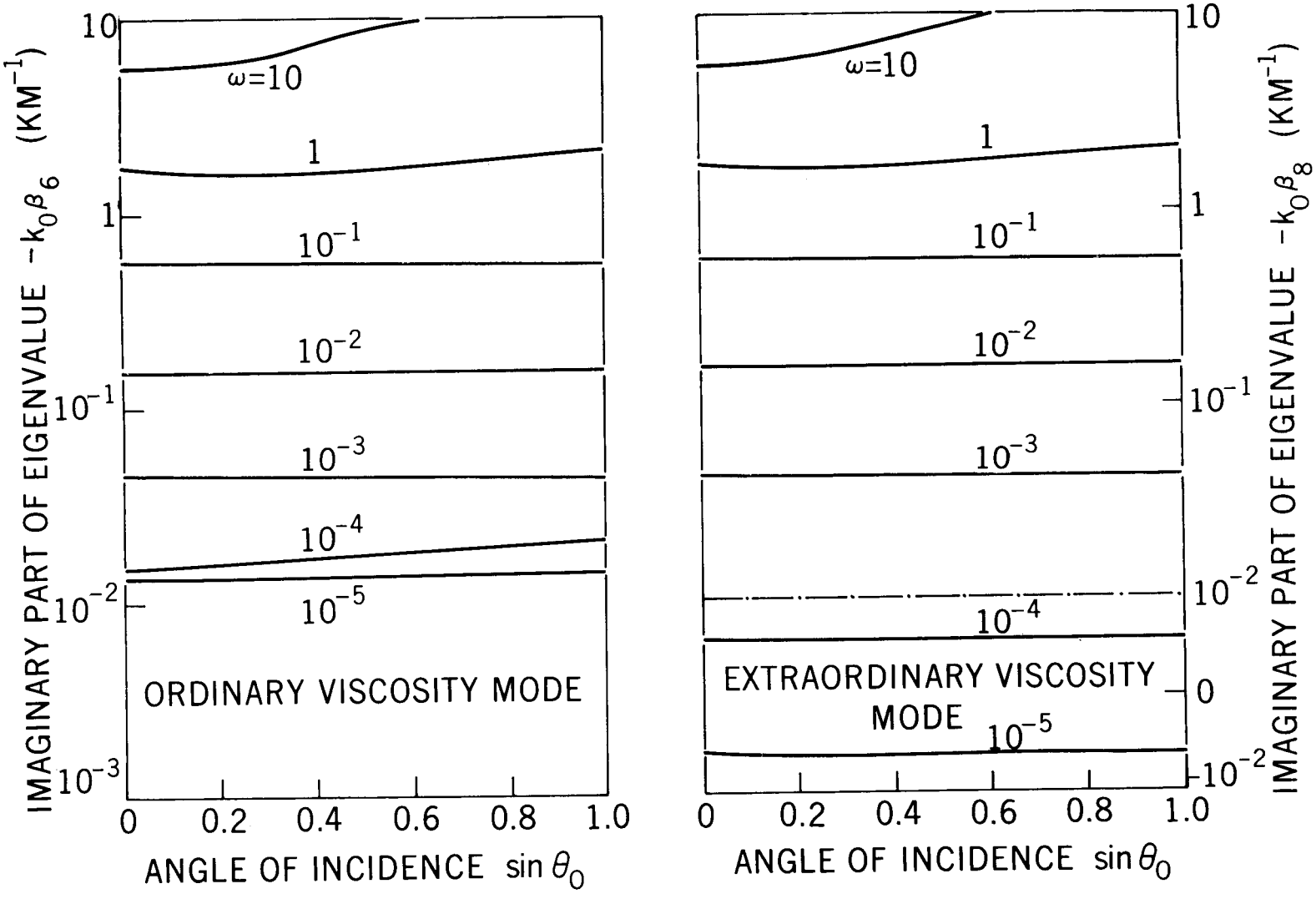

Figure 9–Negative imaginary part $-k_0\beta$ (attenuation factor) of the downgoing ordinary and extraordinary waves. For details see text of figure 8.

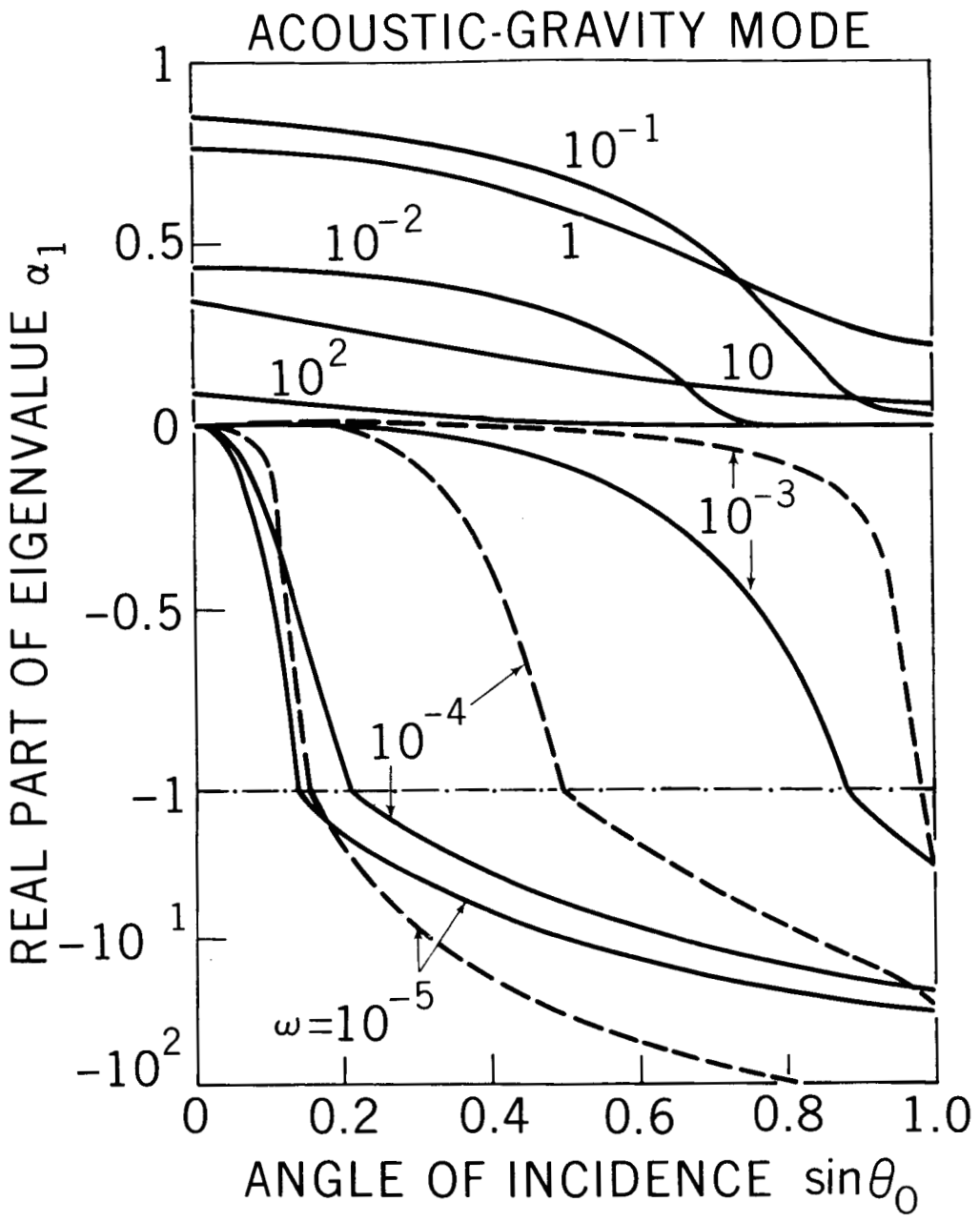

Figure 10–Real part α of the eigenvalue of the upgoing acoustic-gravity waves versus the sine of the angle of incidence θ_0 taking into account heat conduction, molecular viscosity, Coriolis force and ion drag. The parameter is the angular frequency ω (in sec^{-1}). The propagation conditions are: West to east propagation (full lines) and south to north propagation (dashed lines) at the equator. The dash-dotted lines separate different scales.